Base-By-Base Ratcheting of Single Stranded DNA through a Solid-State Nanopore

Binquan Luan, Hongbo Peng, Stas Polonsky, Steve Rossnagel, Gustavo Stolovitzky, and Glenn Martyna

IBM T. J. Watson Research Center, PO Box 218, Yorktown Heights, New York 10598, USA

(Received 11 January 2010; published 10 June 2010)

We investigate the base-by-base translocation dynamics of single-stranded DNA (ssDNA) confined in a solid-state nanopore dressed with an electrostatic trap, using all-atom molecular dynamics (MD) simulation. We observe on the simulation time scale of tens of nanoseconds that ssDNA can be driven through the nanopore in a ratchetlike fashion, with a step size equal to the spacing between neighboring phosphate groups in the ssDNA backbone. A 1D-Langevin-like model is derived from atomistic dynamics which can quantitatively describe simulation results and can be used to study dynamics on longer time scales. The controlled ratcheting motion of DNA could potentially enhance the signal-to-noise ratio for nanoelectronic DNA sensing technologies.

DOI: 10.1103/PhysRevLett.104.238103 PACS numbers: 87.14.gk, 87.15.A−, 87.15.La

The benefits of low-cost, high-throughput human genome sequencing to medical science has inspired extensive experimental [1–4] and theoretical [5,6] work focused on DNA translocation through solid-state nanopores. The integration of nanoelectronic devices to sense each DNA base, could permit DNA sequences to be read out during translocation by the measurement of transverse electrical current [7], voltage signal [8], ionic current [9,10], or hydrogen-bond mediated tunneling signal [11]. One challenge is to develop a scalable and reliable method for controlling the DNA motion [3] to enhance sensing resolution.

Several methods have been suggested to control the motion of DNA in a nanopore including decreasing temperature [12,13], enhancing the electro-osmotic screening of counterions [14–16], increasing the viscosity of an electrolyte [13], using an alternating electric field to drive DNA back and forth [17], and applying magnetic [18] or optical [19] tweezers. Alternatively, it would be useful to force DNA to adopt a ''stop and go'' or base-by-base ratcheting dynamics, analogous to the ''stick-slip'' motion of the atomic force microscope (AFM) tip in a periodic surface potential [20].

Recently, it was proposed [21] that a solid-state nanopore consisting of a metal-insulator-metal sandwich structure [Fig. 1(a)], the ''DNA transistor'', could generate a periodic electric potential for ssDNA. In this Letter, we investigate the ratcheting dynamics of ssDNA, a linear, flexible and charged polymer, in the confined geometry provided by a solid-state nanopore in the presence of said periodic potential. Atomistic MD simulations capable of capturing the details of ssDNA motion are performed; two types of DNA driving methodologies are considered: pulled by a harmonic spring (an *in silico* experiment reminiscent of DNA pulled by an optical tweezer) as an example appropriate for high-resolution single-molecule experimental investigations [19] and pushed by a biasing electric field as an example appropriate for high-throughput sequencing applications [2,3].

Figure 1(a) illustrates the simulation setup. A fragment of ssDNA containing 20 adenine nucleotides poly(dA_{20}) is submerged in a 0.1 M NaCl electrolyte confined inside a 2-nm-radius nanopore. Water molecules are explicitly included. The solid nanopore is cut from an amorphous SiO_2 solid whose position is harmonically constrained in simulations. Periodic boundary conditions are imposed in all three axial directions. The ssDNA is covalently linked to itself over the periodic boundary of the system. As DNA inside a solid-state nanopore can be electrically stretched, the ssDNA in the simulation is put under tension (about a few hundred pico-newtons [22]) by the boundary conditions such that the average spacing d between neighboring phosphate groups is 7.4 Å. Similar results as reported below are obtained in simulation when d is reduced to 6.8 Å. The center of mass of all phosphorus atoms is harmonically constrained near the center of the nanopore. This constraint prevents DNA from being attracted towards the pore surface and can be experimentally realized by polymer-coating the pore [10,23] where we observed the similar ratchetlike dynamics of ssDNA [24]. Two opposite electric fields, $\pm E$ ($E = 108$ mV/Å), are applied [25] in the whole layers aligned with dielectric regions, mimicking the trapping fields in the DNA transistor [Fig. 1(a)]. The thickness of each electrode and each dielectric field region is, respectively, chosen to be $2d$ and $2.5d$, which results in the maximum energy barrier on ssDNA [21].

All-atom MD simulations are carried out in the Bluegene supercomputers using the program NAMD [26], the Amber (parm-bsc0) force field for ssDNA [27], the TIP3P model of water [28] and the standard NVT ($T = 300$ K) simulation procedure [14].

To obtain the mean trapping force exerted on ssDNA, we simulate the pulling of ssDNA by a harmonic spring and measure the force on the spring. An actual experiment using an optical tweezer as a spring is feasible if subnanometer motion of the pulling bead could be resolved [29]. In the simulations, we attach one end of a harmonic spring to the center of mass of all phosphorus atoms (here-

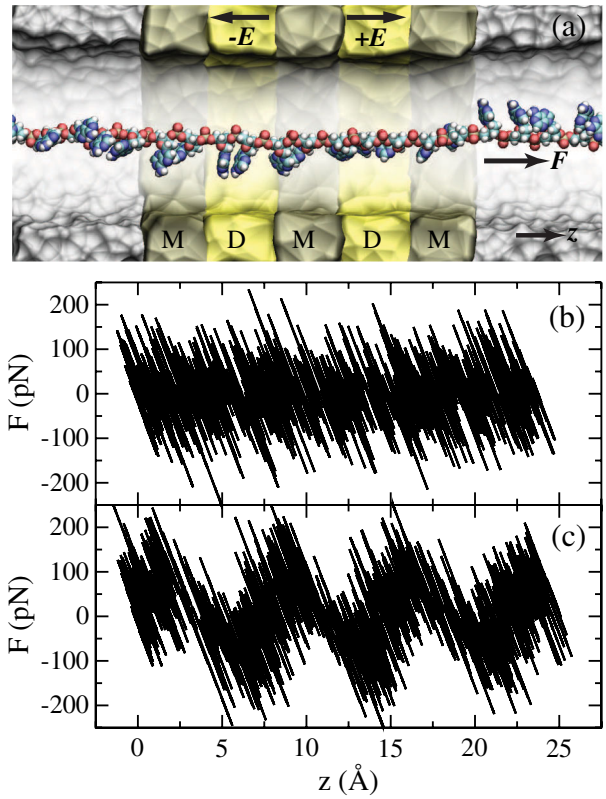

FIG. 1 (color online). Simulations of ssDNA driven through an electrostatic trap in a solid-state nanopore. (a) A cross-section view of the setup of MD simulations. The metal and dielectric regions are labeled with "M" and "D", respectively. (b), (c) Relations between the pulling force and the ssDNA position when ssDNA is pulled at a constant velocity (1 Å/ns) using a harmonic spring (100 pN/Å). The trapping fields are 0 (b) and 108 mV/Å (c), respectively.

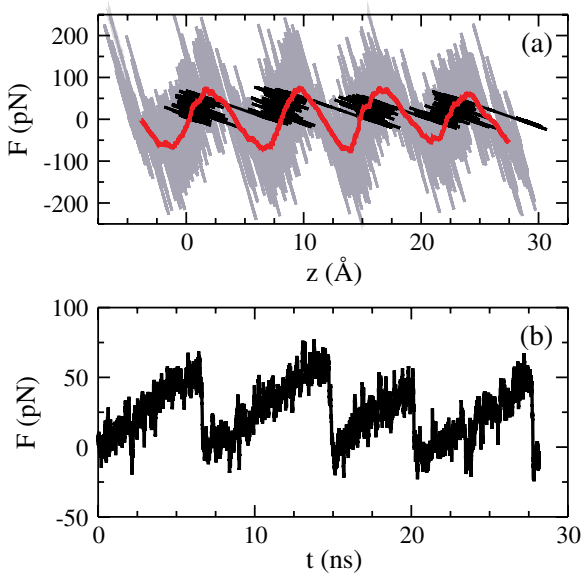

FIG. 2 (color online). Dynamics of ssDNA when pulled using a stiff (100 pN/Å) or a weak (10 pN/Å) spring. (a) Force-position dependence when ssDNA is pulled using the stiff spring [gray line] or the weak spring [black line]. The red curve shows the averaged (over 100 pS) pulling force in the stiff spring. (b) Force-time dependence when ssDNA is pulled using the weak spring.

after called "the ssDNA position") and fix the other end to a pulling stage that moves at a constant velocity v (1 Å/ns). With this setup, the pulling force yields no tension between neighboring nucleotides. Figure 1 shows the pulling force F in the spring versus the ssDNA position before [Fig. 1(b)] and after [Fig. 1(c)] turning on the trapping fields E. When $E = 0$ [Fig. 1(b)], the average force $\langle F \rangle$ in the spring, balancing the hydrodynamic drag force on the DNA, satisfies the relation $\gamma = \langle F \rangle / v$, where the measured friction coefficient γ is about 1 pN · ns/Å. After turning on the trapping field [Fig. 1(c)], the pulling forces in the spring show peaks and valleys separated by a distance d, indicating uphill and downhill "motion" of ssDNA on the landscape of the trapping potential.

The dependence of the instantaneous spring force and the average force on the ssDNA position are shown in more detail in Fig. 2(a). Because of thermal fluctuations, the standard deviation of forces in the spring increases with k and scales like $\sqrt{k_B T k}$, where k_B is the Boltzmann constant, T the temperature and k the spring constant. When pulled by a stiff spring (100 pN/Å), ssDNA follows the pulling stage nearly instantaneously. Therefore, the average force in the spring balances the force of the electric trapping potential. Thus, the curve of the average force [red line in Fig. 2(a)] also illustrates the dependence of the trapping force on the ssDNA position. The maximum trapping force $f^{\max}$ on average is about a half of the theoretical prediction ($eE = 160$ pN) in which the total charge of each nucleotide is assumed to reside at a point [21]. The resulting energy barrier (or trapping energy) is about $5k_BT$.

When the spring constant is reduced to 10 pN/Å, the motion of ssDNA evinces both trapped and slip states of ssDNA [black line in Fig. 2(a)]. Unlike the steady-sliding motion when ssDNA is pulled using the stiff spring [100 pN/Å, grey line in Fig. 2(a)], each slip event corresponds to a hop from an uphill potential surface to the next uphill potential surface. Hopping events are thermally activated if the force in the spring is close to $f^{\max}$. Because of the dissipative hopping process, the average pulling force is nearly always positive [black line in Fig. 2(a)], as opposed to the positive and negative pulling forces observed in the stiff spring case [red line in Fig. 2(a)]. Figure 2(b) shows the time-dependent pulling force, indicating that ssDNA is alternatively in a trapped and a slip states. In a trapped state, ssDNA barely moves forward and the pulling force in the spring builds up. Once the pulling force is big enough for ssDNA to overcome the electric trapping force, ssDNA catches up with the pulling stage (a slip event) and the pulling force in the spring drops.

The simulated ssDNA motion under various pulling conditions is summarized in Fig. 3(a). At the same pulling

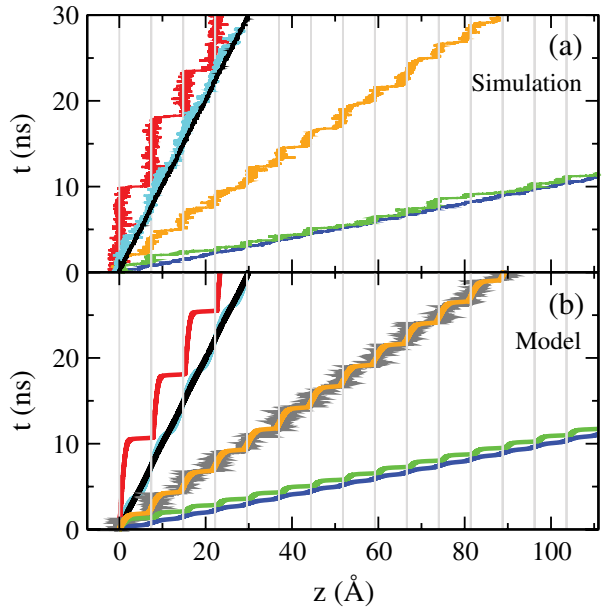

FIG. 3 (color online). Time-position dependence of ssDNA. (a) Simulated time-position dependence of the ssDNA molecule pulled by a harmonic spring. (b) Modeled time-position dependence of the ssDNA molecule that is pulled under the same conditions. According to the pulling velocity, data in each panel are grouped into three sets: (i) $v = 1$ Å/ns and $k = 10$ (red), 100 (cyan), 1000 (black) pN/Å; (ii) $v = 3$Å/ns and $k = 33.3$ (orange) pN/Å; (iii) $v = 10$ Å/ns and $k = 10$ (green), 100 (blue) pN/Å. The interval of mesh lines is d.

velocity ($v = 1$ Å/ns), Fig. 3(a) shows that the motion of ssDNA changes from a steady sliding to a ratcheting motion when the spring constant is decreased. When the pulling velocity is high ($v = 10$ Å/ns), the ratcheting motion is less obvious even when the spring constant is weak ($k = 10$ pN/Å). Together, these results show that the ratcheting motion of ssDNA can be achieved by decreasing the loading rate kv. This is consistent with the fact that the duration, τ, of a trapped state satisfies the relation $\tau \sim f^{\max}/kv$.

To further characterize the ssDNA motion described above, we treat the driven motion of ssDNA along the pore in a thermal bath and on a potential of mean force [30] modeled by $-V_b \cos(2\pi z/d)/2$, using

$$m\ddot{z} = -\gamma\dot{z} - f^{\max}\sin(2\pi z/d) - k(z - z_0) + \sqrt{2\gamma k_B T}\xi, \quad (1)$$

where z is the ssDNA position, m the mass of ssDNA, z_0 ($= vt$) the position of the pulling stage, and ξ the δ-correlated white noise. The external forces exerted on ssDNA are hydrodynamic friction force, electric trapping force and the pulling force from a harmonic spring. According to the measured trapping force shown in Fig. 2(a), we approximate the relation between the trapping force and the ssDNA position using a sinusoidal function with $f^{\max} = V_b\pi/d$. The ssDNA is in the overdamped regime, as dissipation dominates inertia ($\gamma \gg \sqrt{mk}$).

Figure 3(b) shows the solution of the above model [$z(0) = 0$ and $\dot{z}(0) = 0$] without any fitting parameters, when ssDNA is pulled under the same conditions as used in the MD simulations. Predictions of the model at $T = 0$ [smooth lines] and $T = 300$ K [grey line] agree well with the simulation results shown in Fig. 3(a). Because of thermally activated hops in the simulation dynamics [Fig. 3(a)], the duration of the trapped states is not constant at $T = 300$ K in contrast to $T = 0$ [Fig. 3(b)]. As this model accurately captures the dynamics of observed ssDNA motion, the slower motion of ssDNA on the experimental time scale, resulting from employing a slower pulling velocity or a larger trapping force, can be investigated simply by integrating the model (parameterized with coefficients obtained in simulations) to a long time scale.

The observed ratcheting motion of ssDNA depends on the existence of multiple metastable states. In a metastable or a trapped state, $\ddot{z} = \dot{z} = 0$, therefore $-k(x - vt) = f^{\max}\sin(2\pi x/d)$. In Fig. 2(a), the left part of this equation is shown as line segments of the instantaneous force fluctuation of the spring, while the right part is shown as the curve [red line] of the averaged force, or the trapping force. When the spring constant k is bigger than the maximum slope of the curve of the trapping force [red line], each line segment of the force fluctuation intersects the curve of the trapping force only once (i.e., one stable state at any time), indicating that ssDNA moves steadily through the nanopore. However, when k is smaller, some line segments may intersect the curve of the trapping force at several positions, forming several metastable states. A hop between metastable states corresponds to a slip event. Therefore, the criteria for ssDNA to exhibit ratcheting motion is $k < 2\pi f^{\max}/d$, i.e., not only the loading rate kv but also the spring constant k should be less than their respective thresholds.

Using the same atomistic MD simulation setup as above, we remove the pulling spring and replace it by a constant biasing electric field E' across the nanopore. In Fig. 4(a), we show MD trajectories of ssDNA subject to various strengths of the biasing electric field. When ssDNA is driven in the weak biasing electric field [0.6 mV/Å, red line], a ratcheting motion of ssDNA is observed. When the biasing electric field increases, these simulations demonstrate a continuous transition from a ratcheting motion to a steady-sliding motion of ssDNA. A mixing of both types of motion is found at intermediate biasing electric fields. The electrically driven motion of DNA can be effectively modeled using Eq. (1) with the spring force replaced by the constant effective driving force $f_{\text{eff}} = q_{\text{eff}}E'$ [14,16], where q_{eff} is the effective charge of ssDNA.

Figures 4(b)–4(d) show the prediction of Eq. (1) for the time-dependent force in springs with different spring constants. When the spring constant is large [1000 pN/Å, Fig. 4(b)], the spring force balances the modeled sinusoidal trapping force. When $k = 10$ pN/Å [Fig. 4(c)], we obtain

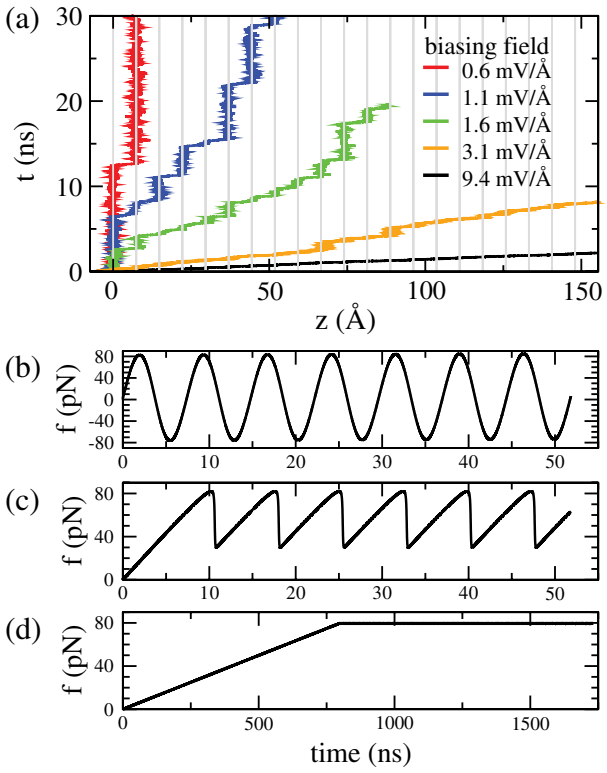

FIG. 4 (color online). Thermally activated ratchetlike motion of ssDNA driven by a biasing electric field. (a) Transition from a ratcheting to a steady-sliding motion of ssDNA when increasing the biasing electric field from 0.6 mV/Å to 9.4 mV/Å, or the electric driving force on bare DNA from 20 to 300 pN. The interval of mesh lines is d. (b)–(d) Predictions of time-dependent force in spring from Eq. (1) at $T = 0$. The spring constants are 1000 pN/Å (b), 10 pN/Å (c), and 0.1 pN/Å (d), respectively. All parameters are the same as used in the simulation.

similar force spikes as shown in the simulation result [Fig. 2(b)] and the motion of DNA is ratchetlike. Each time when the force in spring is big enough to trigger a slip event, ssDNA quickly advances a distance of d and the force in spring drops by kd. In the weak-spring limit [$k = 0.1$ pN/Å], kd is negligible as shown in Fig. 4(d) and spring forces are nearly constant. Thus, electric field driving (or constant force pulling) is the limit of a weak spring pulling. Therefore, similar ratcheting motion of ssDNA is observed when driven by a weak harmonic spring or by a biasing electric field.

In summary, we have investigated the ratcheting motion of ssDNA inside a solid-state nanopore, uncovered the basic mechanism underlying the dynamics and developed a simple 1D-Langevin-like model to describe it. When realized experimentally, this controlled motion of ssDNA could potentially benefit all nanopore-based ssDNA sequencing technologies.

The authors acknowledge useful discussions with Mark Robbins, Ali Afzali, Yuhai Tu, Ajay Royyuru, and Tom Theis. This work was supported by a grant from the National Institutes of Health (R01-HG05110-01).

[1] J. Li, M. Gershow, D. Stein, E. Brandin, and J. A. Golovchenko, Nature Mater. **2**, 611 (2003).
[2] C. Dekker, Nature Nanotech. **2**, 209 (2007).
[3] D. Branton, D. Deamer, A. Marziali, H. Bayley, S. Benner, T. Butler, M. Di Ventra, S. Garaj, A. Hibbs, and X. e. a. Huang, Nat. Biotechnol. **26**, 1146 (2008).
[4] M. Wanunu, W. Morrison, Y. Rabin, A. Y. Grosberg, and A. Meller, Nature Nanotech. **5**, 160 (2010).
[5] K. Luo, T. Ala-Nissila, S. Ying, and A. Bhattacharya, Phys. Rev. Lett. **100**, 058101 (2008).
[6] D. Lubensky and D. Nelson, Biophys. J. **77**, 1824 (1999).
[7] J. Lagerqvist, M. Zwolak, and M. D. Ventra, Nano Lett. **6**, 779 (2006).
[8] M. Gracheva, A. Aksimentiev, and J.-P. Leburton, Nanotechnology **17**, 3160 (2006).
[9] J. J. Kasianowicz, E. Brandin, D. Branton, and D. W. Deamer, Proc. Natl. Acad. Sci. U.S.A. **93**, 13 770 (1996).
[10] S. Iqbal, D. Akin, and R. Bashir, Nature Nanotech. **2**, 243 (2007).
[11] S. Chang, J. He, A. Kibel, M. Lee, O. Sankey, P. Zhang, and S. Lindsay, Nature Nanotech. **4**, 297 (2009).
[12] A. Meller, L. Nivon, E. Brandin, J. Golovchenko, and D. Branton, Proc. Natl. Acad. Sci. U.S.A. **97**, 1079 (2000).
[13] D. Fologea, J. Uplinger, B. Thomas, D. S. McNabb, and J. Li, Nano Lett. **5**, 1734 (2005).
[14] B. Q. Luan and A. Aksimentiev, Phys. Rev. E **78**, 021912 (2008).
[15] S. Ghosal, Phys. Rev. E **76**, 061916 (2007).
[16] S. van Dorp, U. Keyser, N. Dekker, C. Dekker, and S. Lemay, Nature Phys. **5**, 347 (2009).
[17] G. Sigalov, J. Comer, G. Timp, and A. Aksimentiev, Nano Lett. **8**, 56 (2008).
[18] H. Peng and X. Ling, Nanotechnology **20**, 185101 (2009).
[19] U. Keyser, B. Koeleman, S. Dorp, D. Krapf, R. Smeets, S. Lemay, N. Dekker, and C. Dekker, Nature Phys. **2**, 473 (2006).
[20] A. Schirmeisen, D. Weiner, and H. Fuchs, Phys. Rev. Lett. **97**, 136101 (2006).
[21] S. Polonsky, S. Rossnagel, and G. Stolovitzky, Appl. Phys. Lett. **91**, 153103 (2007).
[22] C. Ke, M. Humeniuk, H. S-Gracz, and P. E. Marszalek, Phys. Rev. Lett. **99**, 018302 (2007).
[23] M. Wanunu and A. Meller, Nano Lett. **7**, 1580 (2007).
[24] B. Q. Luan, H. Peng, S. Polonsky, S. Rossnagel, G. Stolovitzky, and G. Martyna (unpublished).
[25] D. B. Wells, V. Abramkina, and A. Aksimentiev, J. Chem. Phys. **127**, 125101 (2007).
[26] J. C. Phillips, *et al.*, J. Comput. Chem. **26**, 1781 (2005).
[27] A. Perez, I. Marchan, D. Svozil, J. Sponer, T. E. Cheatham, C. A. Laughton, and M. Orozco, Biophys. J. **92**, 3817 (2007).
[28] W. L. Jorgensen, J. Chandrasekhar, J. D. Madura, R. W. Impey, and M. L. Klein, J. Chem. Phys. **79**, 926 (1983).
[29] J. Moffitt, Y. Chemla, D. Izhaky, and C. Bustamante, Proc. Natl. Acad. Sci. U.S.A. **103**, 9006 (2006).
[30] R. Zwanzig, in *Nonequilibrium Statistic Mechanics*, (Oxford University Press, New York, 2001).